Hindawi
Shock and Vibration
Volume 2018, Article ID 6839062, 8 pages
https://doi.org/10.1155/2018/6839062

Research Article

A New Erosion Model for Wind-Induced Structural Vibrations

Keqin Yan,[1] **Yi Zhang**,[2,3] **and Tao Cheng**[1]

[1]*School of Civil Engineering, Hubei Polytechnic University, Huangshi, Hubei 435003, China*
[2]*Department of Civil Engineering, Tsinghua University, Beijing 100084, China*
[3]*Geodätisches Institut, Leibniz Universität Hannover, 30167 Hannover, Germany*

Correspondence should be addressed to Yi Zhang; zhang_yi87@163.com

Received 16 March 2018; Revised 7 June 2018; Accepted 17 July 2018; Published 10 September 2018

Academic Editor: Aly Mousaad Aly

In recent years, computational fluid dynamics (CFD) method has been widely utilized in simulating wind-induced snow drifting. In the simulating process, the erosion flux is the main controlling factor which can be calculated by the product of erosion coefficient and the differences between the flow stress and threshold stress. The erosion coefficient is often adopted as an empirical constant which is believed not to change with time and space. However, in reality, we do need to consider the influences of snow diameter, density, and wind speed on the erosion coefficient. In this technical note, a function of air density, sow particle density, snow particle radius, and snow particle strength bond is proposed for the erosion coefficient. Based on an experiment study, the effects of these parameters in erosion coefficient is analyzed and discussed. The probability distribution and value range of erosion coefficient are also presented in this technical note. The applicability of this approach is also demonstrated in a numerical study for predicting the snow distributions around a cube structure. The randomness of the structural vibrations is studied with details.

1. Introduction

In heavy snow areas, wind-induced snow drifting causes unbalanced snowdrift around buildings/on roofs. It is not only difficult to remove but also causes trouble for vehicles and pedestrians. Roof collapse occurs for unbalanced snow distribution.

Wind-induced snow drifting belongs two-phase flow. There are many parameters affecting the result of this phenomenon: wind speed, friction velocity, threshold friction velocity, snow particle radius, density, and cohesion. At present, there are four kinds of research methods for this phenomenon: theoretical analysis, field investigation, wind tunnel (water flume) experiment, and numerical simulation. Field investigation can obtain first hand data, and it is the basis of all other methods. But the field investigation is usually constrained by natural conditions, is time-consuming, and can only obtain the result under certain conditions. Therefore, it is not easy to reveal the inherent law of this phenomenon. Wind tunnel test can change parameters and can make up the shortage of field measurement to some extent. But only a few wind tunnels can carry out this kind of test. Furthermore, similarity criterion is difficult to satisfy due to reduced model. Many former researches have been done on the topic of wind-induced snow drifting through either field experiment [1–8] or numerical simulation [9–13]. Most researchers tried to combine theoretical analysis with empirical formulas from results of field investigations and use it in the numerical simulations [5, 9–13]. In an early works of the authors [14], a new method is developed to measure the air velocity profile surrounding an existing building structure considering snow effects. The snow particle size and its distribution are considered in plotting the velocity profile. In this method, the experiment was conducted based on a simple wind tunnel powered by a fan in the lab. The influences from the field such as the potential damages that might be caused to the equipment due to snow particles are not considered. Different snow size effects are also not catered. Obviously, the input from the field results has a significant influence on the reliability of the analysis. Among these, the modeling of erosion flux is one of the most dominant factors in numerical analysis. Plenty of studies on determining the erosion flux have been carried out in recent years [15].

In these pioneering works, the erosion flux is found to be dependent on the difference between the friction flow stress and threshold friction stress. The erosion flux can be calculated based on the product of a coefficient γ and the stress difference. The determination of the value of γ is based on field experiments. For instance, Schmidt [16] had once carried out experimental tests in a wind tunnel to investigate behavior of drifting spherical glass microbeads, which has a diameter of 350 μm and density of 2.5 g/cm^3. From the experiment, it was found that when flow friction velocity is 0.5 ms^{-1}, γ has a value around 5×10^7 N^{-1}·s^{-1}. It is also reported that the value of coefficient γ increases as the particle diameter decreases. For instance, Anderson [17] carried out investigations with mineral particles in size of sand and found out that the value of γ should be in orders of 10^5 N^{-1}·s^{-1}. Therefore, the particle size is an influential factor in determining the value of γ. In fact, there are more factors that need to be considered in the estimate of γ. The authors believe that it depends on snow conditions.

Since 1990s, computational fluid dynamics (CFD) theory has been brought into the simulation of snow drifting. Similar to the model of Andersen [16], Naaim [11] suggested that the erosion flux of snow can be computed by the product of two factors. The first factor is the difference between the square of flow friction velocity and the square of threshold friction velocity. The second factor is a coefficient ρA, or so-called erosion coefficient A_{ero}, which usually takes a value of 7×10^{-4} kg·m^{-3}. Because of its simplicity, many research works have adopted this concept and taken this value for the erosion coefficient in their CFD simulations [18]. Very limited studies have been carried out to discuss about the value range of this coefficient. And studies on which factors can affect this coefficient are also lacking. Thus, a comprehensive study on the attributes for an erosion coefficient is quite demanding.

The objective of this study was to investigate the value range of erosion coefficient and to derive an expression of erosion coefficient in terms of the dominant factors. Realizing this, the paper is organized as follows. After the introduction, Section 2 will first discuss the dominant factors that are influential to erosion coefficient. Based on these factors, an expression of erosion coefficient is derived. After this, the value range of erosion coefficient is investigated in Section 3. The domain of the dominant factors is considered in this evaluation. The applicability of the developed approach is further demonstrated in a case study carried out in Section 4. The final conclusions drawn from this study are summarized in Section 5.

2. Derivation of the Formula for Erosion Coefficient

As mentioned in many of the literature, coefficient γ, which characterizes the bond strength of snow particles, has the same physical meaning as erosion coefficient A_{ero} in the CFD method [19]. Herein, a short discussion on the relationship between these two coefficients is provided as follows.

In most literature on the topic of wind-induced snow drifting, the snow surface erosion flux is calculated as follows [20]:

$$q_{\text{ero}} = \rho A\left(u_*^2 - u_{*\text{t}}^2\right) = A_{\text{ero}}\left(u_*^2 - u_{*\text{t}}^2\right), \tag{1}$$

where A_{ero} is the erosion coefficient, u_* is the friction velocity, and $u_{*\text{t}}$ is the threshold friction velocity of snow particles. In most former works, the value of A_{ero} is suggested to be 0.0005 or 0.0007.

Later on, Anderson analyzed the characteristics of surface force and suggested that drifted snow particle number should be calculated as follows [9, 17]:

$$N = \gamma\left(\tau - \tau_{\text{t}}\right), \tag{2}$$

where γ is a coefficient characterized by the bond strength between snow particles which usually takes a value of 10^5 N^{-1}·s^{-1}, τ represents the surface shear stress caused by flow, and τ_{t} indicates the threshold shear stress. By combining Equations (1) and (2), the relationship between γ and A_{ero} can be revealed.

The relationship between surface shear stress τ and surface friction velocity u_* can be described by the following equation:

$$u_* = \sqrt{\frac{\tau}{\rho_{\text{a}}}}, \tag{3}$$

where ρ_{a} is the air density (the value usually adopts a value of 1.25 kg·m^{-3} for normal air).

By substituting Equation (3) into Equation (2), we can obtain the following equation for computing the snow particle number:

$$N = \rho_{\text{a}}\gamma\left(u_*^2 - u_{*\text{t}}^2\right). \tag{4}$$

Once the snow particle number is estimated, it can then be used to calculate the erosion flux. Snow surface erosion flux q_{ero} is the drifted snow particle quantity in unit area per unit time. Since drifted snow contains snow particles with different radius, q_{ero} can be expressed as a function of the particle sizes as the following equation:

$$\begin{aligned} q_{\text{ero}} &= \sum_{i=1}^{n} N\rho_{\text{p}i}V_{\text{p}i} = \sum_{i=1}^{n} \frac{\pi d_{\text{p}i}^3}{6}\rho_{\text{p}i}\rho_{\text{a}}\gamma\left(u_*^2 - u_{*ti}^2\right) \\ &= \sum_{i=1}^{n} \frac{4\pi r_{\text{p}i}^3}{3}\rho_{\text{p}i}\rho_{\text{a}}\gamma\left(u_*^2 - u_{*ti}^2\right), \end{aligned} \tag{5}$$

where ρ_{p} is the snow particle density, V_{p} is the snow particle volume, d_{p} is the snow particle diameter, r_{p} is the snow particle radius, and i represents the i_{th} snow particle ($i = 1, 2, \ldots, n$). For simplicity, threshold friction velocity is assumed to be the constant for all snow particles. Thus, Equation (5) can be further revised as follows:

$$q_{\text{ero}} = \sum_{i=1}^{n} \frac{4\pi r_{\text{p}i}^3}{3}\rho_{\text{p}i}\rho_{\text{a}}\gamma\left(u_*^2 - u_{*t}^2\right). \tag{6}$$

Therefore, by substituting Equation (6) into Equation (1), the equation for computing the erosion coefficient can be derived as follows:

$$A_{\text{ero}} = \sum_{i=1}^{n} \frac{\pi d_{\text{p}i}^3}{6} \rho_{\text{p}i} \rho_{\text{a}} \gamma = \sum_{i=1}^{n} \frac{4\pi r_{\text{p}i}^3}{3} \rho_{\text{p}i} \rho_{\text{a}} \gamma. \quad (7)$$

As can be observed from Equation (7), erosion coefficient A_{ero} is a function of snow particle radius and density, coefficient γ, and air density. It is a much more complicated factor which should be quite random depending on snow particle properties. In the following, the influence of different parameters on the erosion coefficient in Equation (7) will be elucidated below.

3. Value Range of Erosion Coefficient

3.1. Randomness of Snow Particle Radius. Wind-induced snow drifting contains snow particles with different radius. Budd [3] analyzed the particle radius distribution through field investigation. He suggested that the drifted snow particle radius obeys two-parameter gamma distribution and gave out the distribution of snow radius along the height Schmidt et al. [21, 22]. A specific formula for this distribution function is given as follows Schmidt [21]:

$$f(r_{\text{p}}) = \frac{r_{\text{p}}^{(\alpha-1)} e^{(-r_{\text{p}}/\beta)}}{\beta^{\alpha} \Gamma(\alpha)}, \quad (8)$$

$$\Gamma(\alpha) = \int_0^{\infty} x^{\alpha-1} \exp(-x)\, dx, \quad (9)$$

$$\alpha = 4.08 + 12.6z, \quad (10)$$

where $f(r_{\text{p}})$ represents the probability density function of snow particle radius, α is the shape parameter of gamma distribution which is proportional to height z from snow surface, β is the scale parameter of gamma distribution, and Γ is a gamma distribution.

It can be seen that α and β are related to average snow radius r_{m} and height z. The relationship among these parameters can be further described by the following equations:

$$\beta = \frac{r_{\text{m}}}{\alpha}, \quad (11)$$

$$r_m = 4.6 \times 10^{-5} z^{-0.258}. \quad (12)$$

It is easy to see from the equation that average snow particle radius r_{m} will decrease as the height z from snow surface increases.

3.2. Randomness of Erosion Coefficient. From the above analysis, we can see the distribution of particle size is highly depending on the height z from snow surface. Snow particle radius varies inversely with z. Tabler's work indicated that when the 10 m height wind speed is less than 12 m/s, saltation is predominant transportation [23]. Bagnold [24] suggested that the height should be within 0.1 meter. Therefore, based on these concerns, in the following part, we only investigate the value range of A_{ero} at three selected heights, namely, $z = 0.02$ m, 0.05 m, and 0.1 m.

To determine the value range of A_{ero}, the calculation is split into four steps. Firstly, based on the surface height value z (0.02 m, 0.05 m, and 0.1 m), the values of α and β are calculated from Equations (10)–(12). Second, based on the values of α and β, the gamma distribution function for the snow particle radius is constructed. Thirdly, substitute the distribution function for snow particle radius $f(r_{\text{p}})$ into Equation (7). By utilizing the kernel smoothing density estimation, probability density distribution function of A_{ero} can be directly obtained (Figure 1(a)). Finally, the cumulative distribution function for erosion coefficient can be derived based on the density function (Figure 1(b)). The comparison between the investigated erosion coefficients at different heights and the reported results in the literature is also illustrated in Figure 1. The estimated statistical parameter values in Figure 1 are recorded in Table 1.

Figure 1(a) shows that the value of A_{ero} concentrates at a value around 1.0×10^{-4}. The probability of values of A_{ero} higher than 2.5×10^{-4} is very small. From the observation of Figure 1(b), we can see that the proposed distribution model has a larger prediction value of erosion coefficient compared to the field experiment results. And this prediction tends to decrease with the increase of surface height. In fact, the model for erosion coefficient at a surface height of 0.05 m has a perfect fit to the results reported in Schmidt [13]. However, on the other hand, results reported in Budd (1966) are more closer to the model predictions for erosion coefficient at a surface height of 0.1 m. This shows how the value of A_{ero} changes with the surface height while considering the randomness in snow particle size.

Besides the effects from randomness of snow particle radius, the erosion coefficient is also largely affected by the snow density ρ_{p} and coefficient γ. Here, a short parametric study is also provided to investigate the influences from these two parameters. In order to have a fair comparison, the surface height in this case is assumed to be unchanged. The values of the gamma distribution parameters are assumed to be constant; for example, $\alpha = 5$ and $\beta = 20$ are adopted in this case, Table 2. Based on Equation (7), a comparison of erosion coefficient for using different snow particle density and snow particle radius is shown in Figure 2. The compared value is the 95 percentile in the distribution function of A_{ero}. It is seen from the figure that when ρ_{p} varies between 300 kg·m^{-3}and 900 kg·m^{-3} and r_{p} varies between 50 μm and 150 μm (common assumption), the value range of A_{ero} is $1.96 \times 10^{-4} \sim 1.6 \times 10^{-3}$. The influence of γ to A_{ero} is also shown in Figure 3. It can be seen from Figure 3 that the influence of coefficient γ to erosion coefficient A_{ero} is quite significant which should not be ignored. However, we have to point out the inherent relationship among snow particle radius, density, and coefficient γ is still not clear yet. In reality, these factors could be dependent on each other. The value range of the erosion coefficient could be enlarged considering a positive dependence in the parameters. Therefore, the results presented here have its limitations. The results are assuming an independent relationship among the

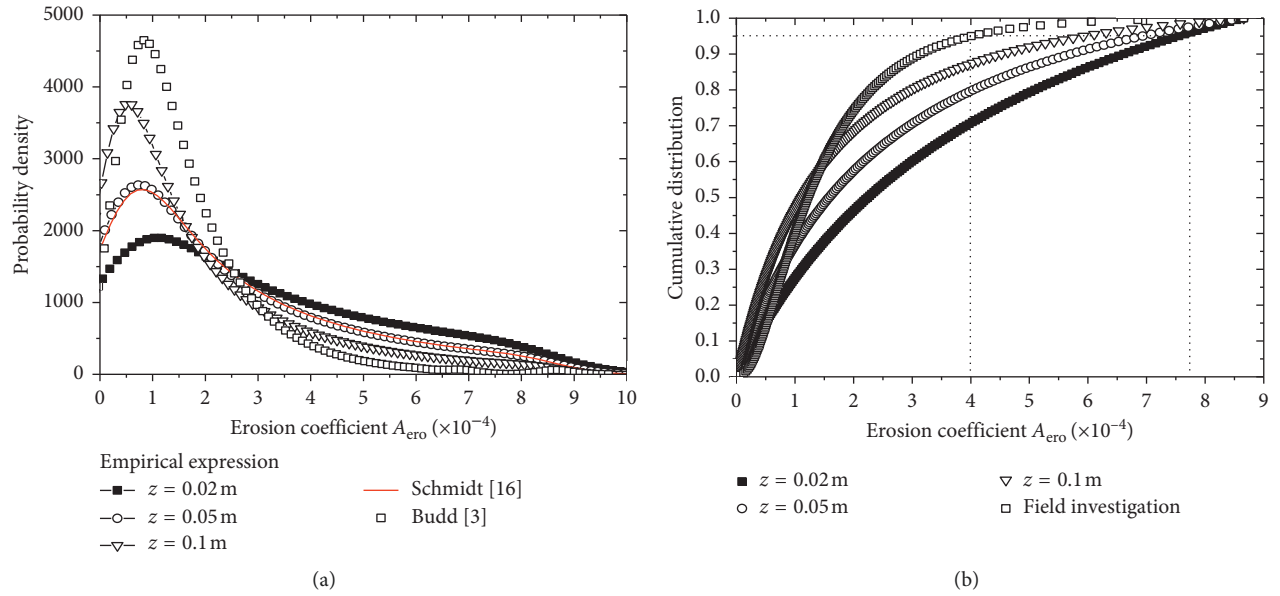

Figure 1: (a) Probability density distribution of A_{ero} and (b) cumulative distribution of A_{ero}.

Table 1: Parameter values in Figure 1.

Parameter	Surface height z (m)			Budd [3]	Schmidt [13]
	0.02	0.05	0.1		
α (m)	4	4.7	6	15	5
β	30	21	15	4	20
r_m (μm)	120	100	90	80	100

Note: $\rho_a = 1.25\,\text{kg}\cdot\text{m}^{-3}$, $\rho_p = 500\,\text{kg}\cdot\text{m}^{-3}$, $\gamma = 10^5\,\text{N}^{-1}\cdot\text{s}^{-1}$, $r_p = (1\sim150)\,\mu$m.

Table 2: Parameter values in Figures 2 and 3.

α (m)	β	r_m (μm)	ρ_p (kg·m^{-3})	ρ_a (kg·m^{-3})	γ (N^{-1}·s^{-1})	r_p (μm)
5	20	50~150	300~900	1.25	10^5~10^7	50~150

considered parameters. It should be further validated through field investigation while considering all physical reasons about the parameter interactions.

4. Case Study: Prediction of Snow Distribution around Cube Structure

To demonstrate the applicability of the proposed model for erosion coefficient, this section will conduct a case study on a real engineering snow problem. In this case study, the objective is to predict the snow distribution around a cube structure when there is snow drifting. As discussed in the former section, erosion coefficient changes with different snow conditions. Therefore, herein, we considered two different snow conditions, namely, fresh snow condition and old snow condition, in the analysis. The field experiment has already been carried out by authors in 2009 in Harbin [7, 25]. These results will be used as a reference to compare with the numerical analysis in this paper.

4.1. Numerical Model Analysis. In order to put in the model of erosion coefficient, the numerical model for the problem is established first. The computational domain and meshing are constructed at a model scale which is exactly corresponding to the field investigation. The dimensions of the cube structure model are $0.2 \times 0.2 \times 0.2\text{m}^3$ ($H = 0.2$ m). The dimension of the simulation domain is $3.2\times\ 1.2 \times 1.2\ \text{m}^3$. The meshing of the model includes 2096000 hexahedral elements. The minimum volume of the elements is $1.357 \times 10^{-6}\,\text{m}^3$, while the maximum volume of the element is $2.26 \times 10^{-6}\,\text{m}^3$. The details of the meshing are illustrated in Figure 4.

The inlet of the simulation domain adopted velocity inlet boundary. The wind-velocity profile inside the simulation domain is defined based on the logarithmic law as follows:

$$u(z) = \frac{u_*}{k} In\left(\frac{z + z_0}{z_0}\right), \tag{13}$$

where z_0 is the roughness height which can be determined from the field experiment (in this case, $z_0 = 0.2$ mm) and u_*

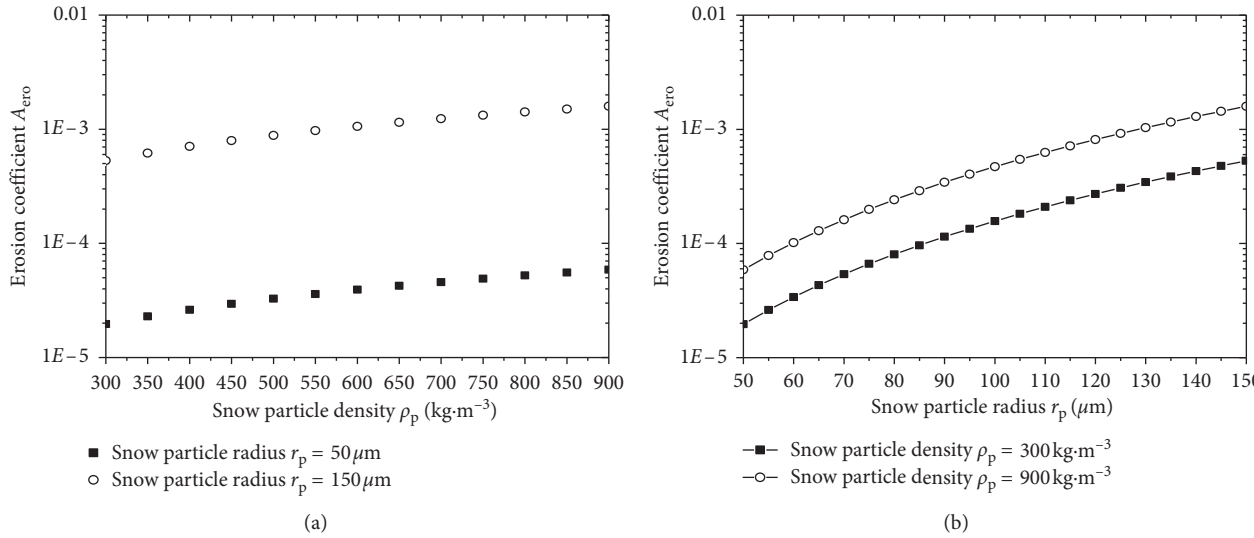

Figure 2: (a) Relationship between A_{ero} (95 percentile) and ρ_p and (b) relationship between A_{ero} (95 percentile) and r_p.

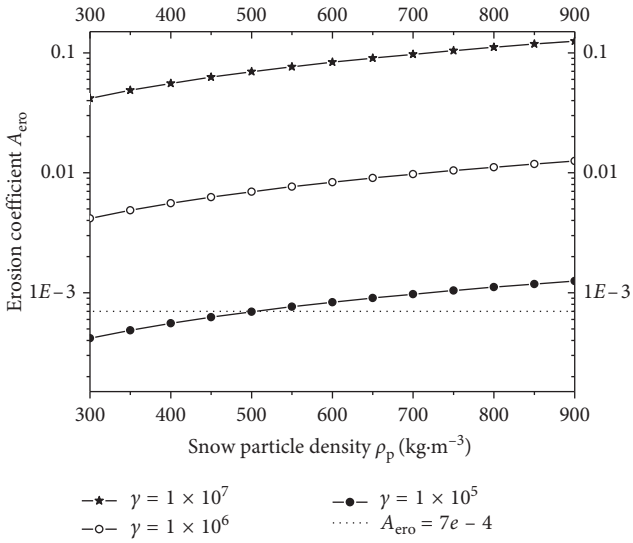

Figure 3: Relationship between A_{ero} and γ.

is the friction velocity which can be determined based on the values of u_{ref} and z_{ref} (0.2 m) from the field experiment. Furthermore, k is the von Karman constant (0.42) and z is the height coordinate. The turbulent kinetic energy K is calculated from the mean wind speed and the measured turbulence intensity using the following equation:

$$K(z) = \alpha\left[I_u(z)u(z)\right]^2, \tag{14}$$

where I_u is the measured streamwise turbulence intensity and α is a parameter ranging from 0.5 to 1.5 [14]. In this study, a value of 1.5 is adopted for α. The turbulence dissipation rate ε can be estimated by the following equation:

$$\varepsilon = \frac{u_*^3}{k(z + z_0)}. \tag{15}$$

Therefore, based on the model, the vertical profiles of $u(z)$ and I_u inside the simulation domain and around the cube structure (incident profiles) are simulated and calculated (Figure 5).

The simulation domain is assumed to be symmetric along the vertical and horizontal directions. The surface of the cube structure is assumed to be stationary walls. The commercial CFD code, ANSYS Fluent 15, is used to perform the simulations. UDF files are added to simulate snow drifting. The 3D steady Reynolds-averaged Navier–Stokes (RANS) equations are solved in combination with the $k-\varepsilon$ model. The SIMPLE algorithm is used for pressure-velocity coupling. The pressure interpolation applied here is second order. Convergence is assumed to be obtained when all the scaled residuals leveled off and reached a minimum of 10^{-6} for x, y, and z momentum, 10^{-4} for k and ε.

4.2. Results and Discussion

Figure 6 shows the results of numerical simulation and field investigation for the investigated problem with consideration of fresh snow. The values of parameters for this simulation are shown in Table 3. Figure 7 shows the results of numerical simulation and field investigation for the same problem with consideration of old snow condition which was compressed by wind. The values of parameters for this simulation are shown in Table 4.

The values of snow radius, density, and threshold friction velocity in Tables 3 and 4 are based on field investigation [7]. The value of γ is taken from the suggested value provided by Schmidt and Shoa [15, 16]. Therefore, erosion coefficient can be calculated based on these parameters and the developed method. In this study, erosion coefficient for fresh and dry snow is about 10^{-3} and 7×10^{-4} for old and wind compressed snow. The results showed that the numerical predictions can accurately depict the real phenomenon. The difference of snow distribution between numerical simulation and field investigation is quite small, indicating the applicability of the proposed approach. Meanwhile, from the observation of Figures 6 and 7,

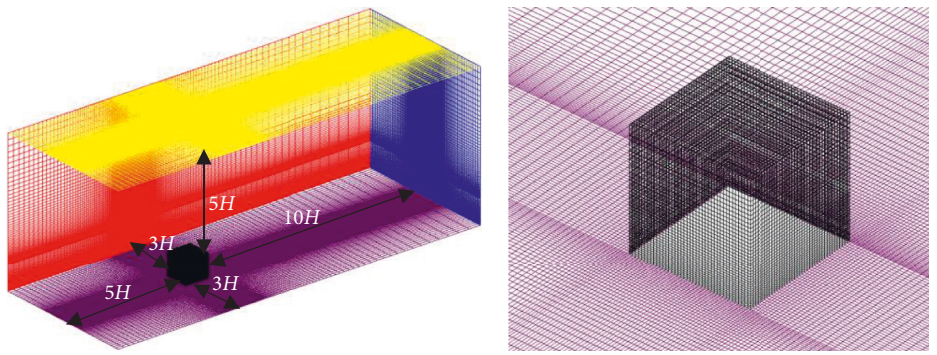

(a) (b)

Figure 4: Perspective view and meshing of simulation domain and cube structure: (a) perspective view of the simulation domain and (b) meshing around the cube structure.

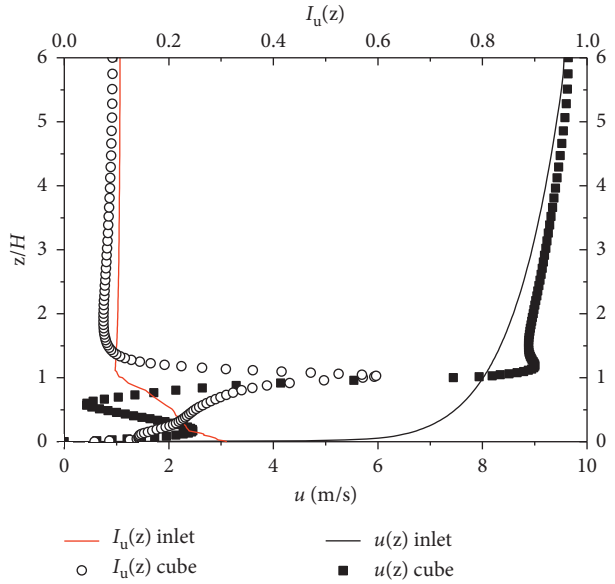

Figure 5: Profiles of the mean wind speed (u) and turbulent kinetic energy (K).

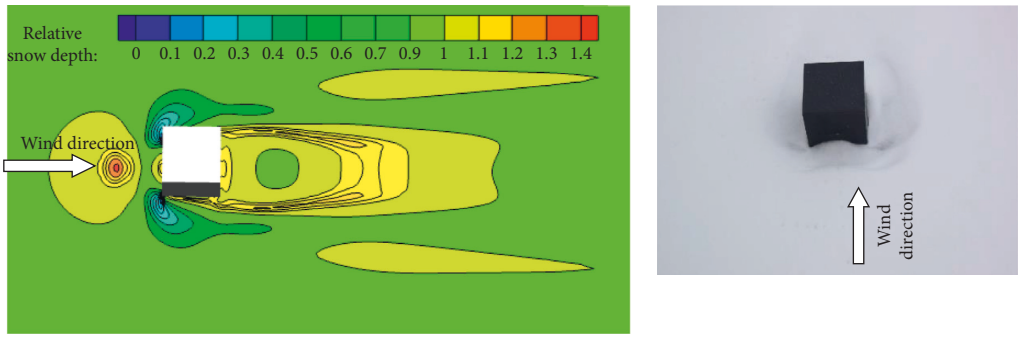

(a) (b)

Figure 6: (a) Numerical simulation and (b) field investigation of snow distribution around a cube structure with fresh and dry snow.

it should be noticed that the snow condition has a significant influence on the snow distribution. This is mainly due to the differences in erosion coefficient. The value of erosion coefficient is largely depending on the snow property parameters. It further proves that we should not use the same erosion coefficient for different snow conditions.

Table 3: Parameter values for simulating fresh and dry snow.

Parameters	r (μm)	ρ_a (kg/m^3)	ρ_p (kg/m^3)	γ (N^{-1}·s^{-1})	u_{*t} (m/s)	t (s)
Value	100	1.25	170	10^6	0.2	240

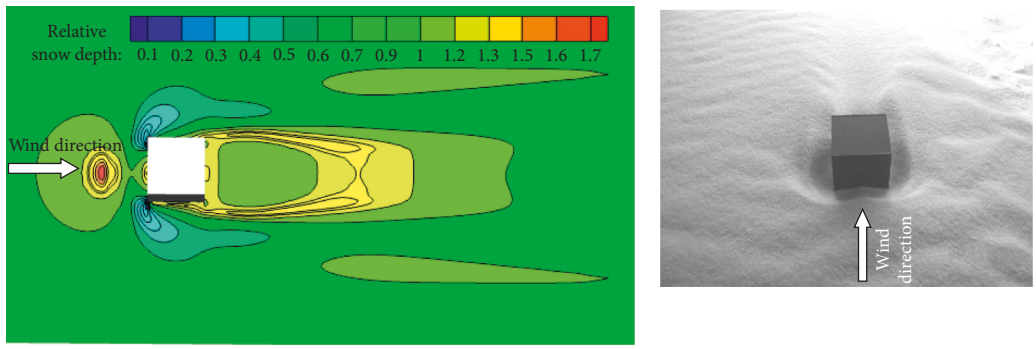

(a) (b)

Figure 7: (a) Numerical simulation and (b) field investigation of snow distribution around a cube structure with old and wind exposed snow.

Table 4: Parameter values for simulating old and wind compressed snow.

Parameters	r (μm)	ρ_a (kg/m^3)	ρ_p (kg/m^3)	γ (N^{-1}·s^{-1})	u_{*t} (m/s)	t (s)
Value	150	1.25	400	10^5	0.35	3600

5. Conclusion

In this technical note, a study on the determination of erosion coefficient is provided. Several parameters which are quite influential to erosion coefficient are being investigated. This includes air density ρ_a, snow particle density ρ_p snow radius r_p, and experiment coefficient γ. An equation of calculating the erosion coefficient for considering these important parameters is derived. By considering the randomness of snow radius, the randomness and value range of erosion coefficient are presented. A case study is conducted to demonstrate the applicability of the proposed approach. It was found that the developed approach can give a perfect prediction of the snow distribution when it is compared to the field investigation. And results showed that the erosion coefficient is very sensitive to the snow conditions. However, the dependences among snow parameters are not considered in this paper. The conclusions and results drawn from this technical note have to be used in view of these limitations. Future work should be put on the investigation of the importance of parameter dependences to the erosion coefficient.

Notations

A_{ero}: Snow surface erosion coefficient (kg·m^{-3})
d_p: Diameter of snow particle (m)
g: Acceleration of gravity (m·s^{-2})
N_a: Drifting snow particles in unit horizontal area per unit time (m^{-2}·s^{-1})
$q_{ero}(x)q_{dep}(x)$: Erosion/deposition flux (kg·m^{-2}s^{-1})
r_p: Radius of snow particles (m)
u_{10}: 10 m wind velocity (m·s^{-1})
u_{ref}: Average wind velocity at reference height (m·s^{-1})
u_*, u_{*t}: Friction velocity and threshold friction velocity of surface (m·s^{-1})
V_p: Volume of snow particle (m^3)
w_f: Settle velocity of snow particle (m·s^{-1})
α: Shape parameter of gamma distribution (m)
β: Length scale parameter of gamma distribution (dimensionless)
Γ: Gamma distribution
ρ_a: Air density (kg·m^{-3})
ρ_p: Snow particle density (kg·m^{-3})
τ: Shear stress of snow surface (N·m^{-2})
τ_t: Threshold shear stress of snow surface (N·m^{-2})
υ: Viscosity coefficient of air motion (m^2·s^{-1})
μ: Aerodynamic coefficient of viscosity (kg·m^{-2}s^{-1})
γ: Experimental constant (N^{-1}·s^{-1}).

Data Availability

The data used to support the findings of this study are available from the corresponding author upon request.

Conflicts of Interest

The authors declare that there are no conflicts of interest regarding the publication of this paper.

Acknowledgments

This research was supported by the Innovation Foundation in Youth Science and Technology Team of Hubei Province (no. T201823), 2017 Provincial Teaching Reform Research Project (no. 2017A09), Hubei Polytechnic University Talent Introduction Project (no. 13xjz07R), Natural Science Fund of Hubei Province (2012FKC14201 and 2013CFC103), Scientific Research Fund of Hubei Provincial Educational Department (no. D20134401), and Innovation Foundation in Youth Team of Hubei Polytechnic University (no. Y008).

References

[1] R. A. Bagnold, *The Physics of Blown Sand and Desert Dunes*, Methuen, London, UK, 1941.

[2] J. H. M. Beyers, P. A. Sundsbø, and T. M. Harms, "Numerical simulation of three-dimensional, transient snow drifting around a cube," *Journal of Wind Engineering & Industrial Aerodynamics*, vol. 92, no. 9, pp. 725–747, 2004.

[3] W. F. Budd, *The Drifting of Nonuniform Snow Particles, Studies in Antarctic Meteorology*, American Geophysical Union, Washington, DC, USA, 2013.

[4] P. Delpech, P. Palier, and J. Gandemer, "Snowdrifting simulation around Antarctic buildings," *Journal of Wind Engineering and Industrial Aerodynamics*, vol. 74–76, pp. 567–576, 1998.

[5] R. S. Anderson and P. K. Haff, "Wind modification and bed response during saltation of sand in air," *Acta Mechanica Supplementum*, vol. 1, no. 1, pp. 21–51, 1991.

[6] Y. Zhang, C. W. Kim, M. Beer, H. Dai, and C. G. Soares, "Modeling multivariate ocean data using asymmetric copulas," *Coastal Engineering*, vol. 135, pp. 91–111, 2018.

[7] Y. Shoa, "Numerical modelling of saltation in the atmospheric surface layer boundary-layer meteorology layer," *Boundary-Layer Meteorology*, vol. 91, no. 2, pp. 199–225, 1999.

[8] F. Naaim-Bouvet, H. Bellot, K. Nishimura et al., "Detection of snowfall occurrence during blowing snow events using photoelectric sensors," *Cold Regions Science and Technology*, vol. 106-107, pp. 11–21, 2014.

[9] F. Naaim-Bouvet and P. Mullenbach, "Field experiments on "living" snow fences," *Annals of Glaciology*, vol. 26, pp. 217–220, 1998.

[10] M. Naaim, F. Naaim-Bouvet, and H. Martinez, "Numerical simulation of drifting snow: erosion and deposition models," *Annals of Glaciology*, vol. 26, pp. 191–196, 1998.

[11] M. O'rourke, A. Degaetano, and J. D. Tokarczyk, "Snow drifting transport rates from water flume simulation," *Journal of Wind Engineering & Industrial Aerodynamics*, vol. 92, no. 14-15, pp. 1245–1264, 2004.

[12] T. Okaze, Y. Takano, A. Mochida, and Y. Tominaga, "Development of a new k–ε model to reproduce the aerodynamic effects of snow particles on a flow field," *Journal of Wind Engineering and Industrial Aerodynamics*, vol. 144, pp. 118–124, 2015.

[13] R. Schmidt, "Vertical profiles of wind speed, snow concentration, and humidity in blowing snow," *Boundary-Layer Meteorology*, vol. 23, no. 2, pp. 223–246, 1982.

[14] K. Yan, T. Cheng, and Y. Zhang, "A new method in measuring the velocity profile surrounding a fence structure considering snow effects," *Measurement*, vol. 116, pp. 373–381, 2018.

[15] R. A. Schmidt, "Estimates of threshold windspeed from particle sizes in blowing snow," *Cold Regions Science and Technology*, vol. 4, no. 3, pp. 187–193, 1981.

[16] R. A. Schmidt, "Measuring particle size and snowfall intensity in drifting snow," *Cold Regions Science and Technology*, vol. 9, no. 2, pp. 121–129, 1984.

[17] Y. Shao and A. Li, "Numerical modelling of saltation in the atmospheric surface layer," *Boundary-Layer Meteorology*, vol. 91, no. 2, pp. 199–225, 1999.

[18] P.-A. Sundsbø, "Numerical simulations of wind deflection fins to control snow accumulation in building steps," *Journal of Wind Engineering and Industrial Aerodynamics*, vol. 74–76, pp. 543–552, 1998.

[19] R. D. Tabler, *Snow Fence Handbook: (Release 1.1)*, Tabler & Associates, Niwot, CO, USA, 1988.

[20] T. K. Thiis, "Large scale studies of development of snowdrifts around buildings," *Journal of Wind Engineering and Industrial Aerodynamics*, vol. 91, no. 6, pp. 829–839, 2003.

[21] Y. Tominaga, A. Mochida, R. Yoshie et al., "AIJ guidelines for practical applications of CFD to pedestrian wind environment around buildings," *Journal of Wind Engineering and Industrial Aerodynamics*, vol. 96, no. 10-11, pp. 1749–1761, 2008.

[22] Y. Tominaga, T. Okaze, and A. Mochida, "CFD modeling of snowdrift around a building: an overview of models and evaluation of a new approach," *Building and Environment*, vol. 46, no. 4, pp. 899–910, 2011.

[23] T. Uematsu, T. Nakata, K. Takeuchi, Y. Arisawa, and Y. Kaneda, "Three-dimensional numerical simulation of snowdrift," *Cold Regions Science and Technology*, vol. 20, no. 1, pp. 65–73, 1991.

[24] B. R. White and J. C. Schulz, "Magnus effect in saltation," *Journal of Fluid Mechanics*, vol. 81, no. 3, pp. 497–512, 1977.

[25] A. Winstral, D. Marks, and R. Gurney, "Simulating wind-affected snow accumulations at catchment to basin scales," *Advances in Water Resources*, vol. 55, pp. 64–79, 2013.